MADRID 2015
1-4 June 2015 | IFEMA Madrid

Tu P6 11

Ray-tracing-based Input Data Selection RTM - A Target Oriented Approach for Clearer Subsalt Image

C. Peng* (CGG Services (US) Inc), W. Gou (CGG Services (US) Inc) & G. Liu (CGG Services (US) Inc)

SUMMARY

We present an input data-selection workflow based on 3D ray-tracing to improve the reverse time migration image in areas of poor illumination and low signal-to-noise ratio. It is effective for imaging subsalt three-way closure with weak subsalt primaries and strong noise levels. The workflow can be applied to any type of survey, but it is most suitable for full azimuth geometries. We focused on data selection using 3D ray-tracing, but this workflow can be easily adapted to use finite-difference wave-equation modelling. The data selection information can either be used to scale up weak primary signal before migration or to be migrated separately and merged into a full migration result in the post-migration stage.

Introduction

Many areas in the Gulf of Mexico (GOM) are characterized by very complex salt geometry, which makes processing and imaging those areas challenging. To improve the illumination under these salt bodies, acquisition technologies have evolved significantly from narrow-azimuth (NAZ) to wide-azimuth (WAZ) and, more recently, to full-azimuth (FAZ) geometries with ultra-long offsets (Mandroux et al. 2013). The processing results of these surveys have shown that FAZ data provide the best chance to illuminate difficult subsalt targets (e.g., subsalt steep dips, three-way structural closures).

However, even with FAZ geometry, some subsalt reflectors are illuminated only by small ranges of subsurface azimuths or reflection angles. Coherent noise such as mode-converted waves and residual multiples can easily be 20 dB stronger than the subsalt signals. In addition, with an imperfect velocity model, such as in the areas with complex salt geometry that need intensive interpretation work or shale zones with weak reflections where tomography has fewer constraints, the primary signals can easily introduce migration swings on weak target events. In these cases, more data does not guarantee a better image. That led to the emergence and re-emergence of approaches to boost signals while suppressing subsalt noise (Nemeth et al. 1999; Shen et al. 2011; Li et al. 2012; Chazalnoel et al. 2012).

We present an input data-selection workflow based on 3D ray-tracing to improve the reverse time migration (RTM) image in areas of poor illumination and low signal-to-noise ratios (S/N). This workflow effectively images subsalt three-way closures with weak subsalt primaries and strong noise levels. With a quick turnaround time, this workflow can be used iteratively to optimize the target image or as a tool to help salt scenario testing. It can be applied to any type of survey, but it is most suitable for FAZ geometry because there is a greater chance of selecting the correct shot-receiver pairs. Although similar to the visibility analysis done by Jin and Xu (2010), it is implemented in a more quantitative way and in a different direction. Instead of guiding the optimization of acquisition parameters, the workflow is designed to extract every available bit of useful signal available to improve subsalt imaging of a particular target area. While we mainly discuss data selection using 3D ray-tracing, this workflow could easily be adapted for finite-difference wave-equation modelling (WEM) (personal communication with Yi Huang and Chu-Ong Ting). The data-selection information from 3D ray-tracing or WEM can be used to scale up weak primary signal before migration, or to migrate separately and merge the results into the full migration result in the post-migration stage.

Method and synthetic example

The workflow of 3D ray-tracing based data selection can be broken down into the following six steps:

1) Produce RTM stack image with all of the data using a salt body velocity model.
2) Interpret target horizons based on the full input RTM image.
3) Run 3D ray-tracing using the same velocity model to get all the successful rays (shot/receiver pairs).
4) Generate illumination QC products (e.g., shot foldmap, reflector hitmap, and Rose diagram).
5) Use the information from Step 4 to select a portion of the data (on both shot and receiver sides) that contributes to the target reflector for migration.
6) Migrate the selected data and merge the output volume into the full migration.

If the target event is not fully consistent with the interpreted horizons in the new RTM volume, the interpreter can restart the process at Step 2 and refine the target horizon based on the new image. The above steps can be performed iteratively until the interpreter is satisfied with the final image.

We first tested this workflow on 3D synthetic data with free-surface multiples from the SEG Advanced Modelling Program. The shots and receivers of the synthetic modelling were defined in a staggered acquisition with FAZ coverage up to a 10 km range and 18 km maximum offsets (Mandroux et al. 2013). The receiver depth was constant for simplicity.

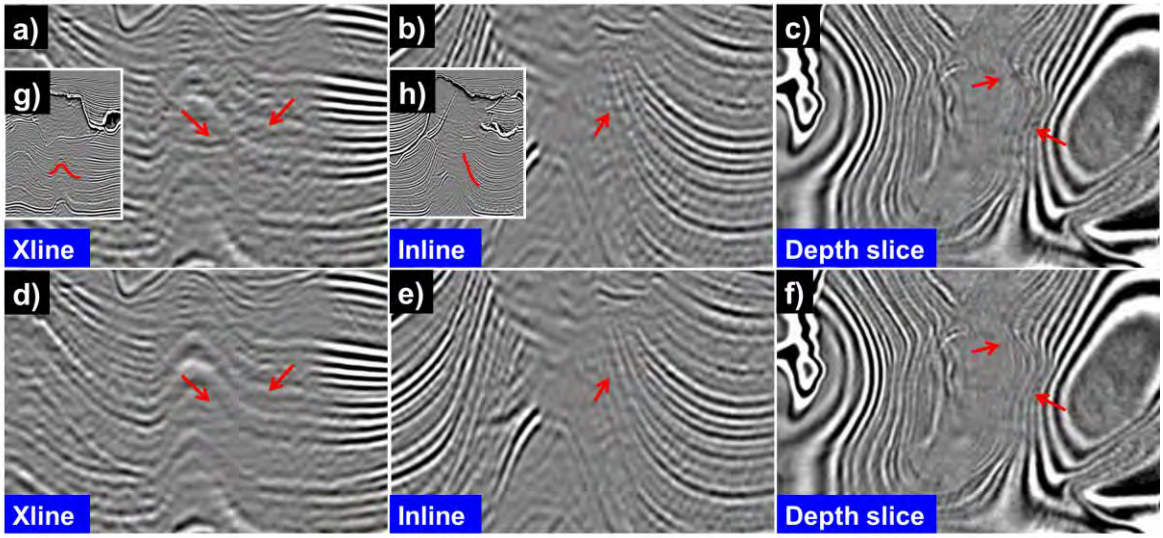

Figure 1 *Full input reverse time migration (RTM) in (a) crossline view, (b) inline view, and (c) depth slice. Merged RTM incorporating selective migration in (d) crossline view, (e) inline view, and (f) depth slice. The inset (g) shows the location of the target horizon at the inline view, and inset (h) shows the location of the target horizon at the crossline view.*

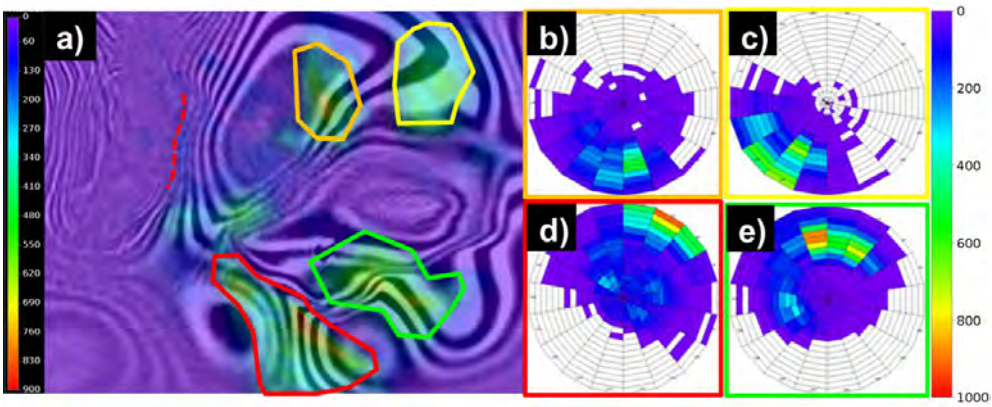

Figure 2 *(a) Shot foldmap of the target event (dashed horizon in red) and Rose diagrams calculated from shots inside (b) orange polygon, (c) yellow polygon, (d) red polygon, and (e) green polygon.*

The steeply dipping events were heavily contaminated by noise, especially in the crossline direction (Figure 1a). We interpreted the target event (red horizon in Figures 1g and 1h) on the full input RTM and performed 3D ray-tracing with predefined shot/receiver grids on the surface (i.e., the modelling grid is the same as the acquisition grid). Figure 2a shows the shot foldmap as colour attributes overlaying the seismic depth slice, while Figures 2b-2e show four Rose diagrams calculated from shots inside the different polygons. The Rose diagrams indicate that the azimuthal distributions and offset ranges are different for each of the four shot clusters. This example also shows that, for complicated structures, different parts are illuminated by different azimuths; only a FAZ survey can illuminate the entire structure. If we only had an east-west direction WAZ survey, due to the short offset coverage in the north-south direction, the target area would have very limited illumination. Even by performing the same data selection approach on the WAZ survey, very few shot/receiver pairs would be chosen for migration, and a limited benefit would be expected.

We chose the shot/receiver pairs based on this information and then ran a selective input migration. The shot foldmap shows the identified shot locations, and the Rose diagrams show the azimuthal distribution and offset ranges of receiver locations (Figure 2). We then merged the selective migration RTM volume with the full migration RTM stack using a flow similar to merging vector offset outputs

(Xu et al. 2011) (Figures 1d-1f). Compared to the full input RTM stack (Figures 1a-1c), the merged volume (Figure 1d-1f) shows a much clearer image at the steeply dipping three-way closure.

Examples with field data

To further evaluate the workflow, we applied our workflow to field data covering approximately 600 sq. km in Keathley Canyon, Gulf of Mexico. The data were acquired from a FAZ survey in staggered geometry with 18 km maximum offsets and variable-depth streamers. Based on the geology, we determined there is likely a three-way truncation against the salt and thus performed an input data-selection RTM. After several iterations of selective migrations, we observed a clearer three-way truncation, and the new image became consistent in both inline and crossline views (Figures 3b and 3d). These steeply dipping truncations are not seen in the full input RTM because they are masked by coherent noise (e.g., mode converted waves, residual multiples) associated with shallower strong reflectors (top of salt and base of salt). Because the target events are dipping in the opposite direction from the noise generators, they are illuminated from opposite directions. By using data-selection input, we isolated the weak useful signal from the high amplitude coherent noise at the input stage and the migration volume after selection revealed the weak events.

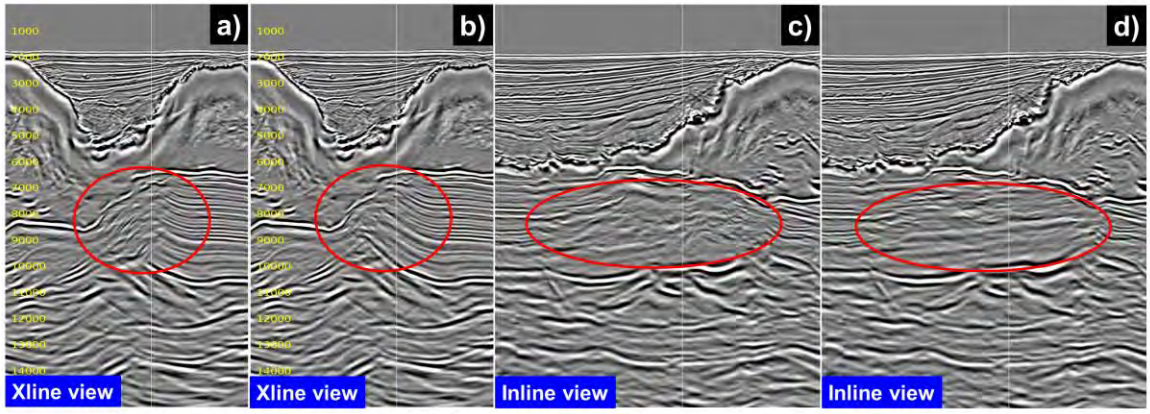

Figure 3 *RTM stack image. (a) With full input in crossline view. (b) Including selective migration in crossline view. (c) With full input in inline view. (d) Including selective migration in inline view.*

Sensitivity analysis

To see what happens if the interpreted horizon is off from the true reflectors, we performed a sensitivity analysis on our workflow. A synthetic three-way closure model was created with a complicated salt geometry, including salt wings, dirty salt, and sediment inclusions. Using this model, we performed a 3D acoustic finite difference modelling and migrated the output with RTM (Figure 4). Besides the true dip, we used different dips of horizons to select the input data for migration. Figures 4b-4e show that data-selection RTM greatly attenuates noise and enhances signal. Even if the interpreted horizon was inconsistent with the true reflector dip, the selective migration still produced the event with the correct dip but with slightly weaker amplitude. This study demonstrates that the workflow has some tolerance, and even though the exact reflector shape may be unknown for some targets before selective migration, we can still interpret the target horizon based on the best RTM image and complete the workflow. Once the new RTM image shows a better defined target, we can adjust the interpreted horizon for an even better result.

Discussions and conclusions

We presented a data-selection workflow based on 3D ray-tracing to improve the subsalt image. The workflow can be performed iteratively so that a very accurate estimate of the target structures is not needed to start. It can greatly improve the image at subsalt three-way closures with weak subsalt primaries and strong noise levels as well as at difficult salt base. Because of the short turnaround time,

it can also be used as a tool to help salt scenario testing. Due to poor illumination at subsalt area, it is most suitable for FAZ data. In some cases, more data and more azimuths do not guarantee a better image, but by using the data-selection process, the potential of FAZ coverage can be fully used.

The data-selection approach can also be adapted to use WEM, which might benefit areas that have very complicated salt geometries or that are mainly illuminated by multiple-bounce reflections and prismatic waves, with an expense of longer turnaround time. Because the salt geometry is complex in the field data example (Figure 3), we have also tried WEM for input data selection, and the result is very close to using ray-tracing in this case.

The workflow has some limitations. Although some error tolerance in the target interpretation is acceptable, it requires good knowledge of the target structure. The workflow requires some manual work and is limited to a localized area. It might enhance some unwanted non-specular energy, especially at the boundary or outside the interpretation area.

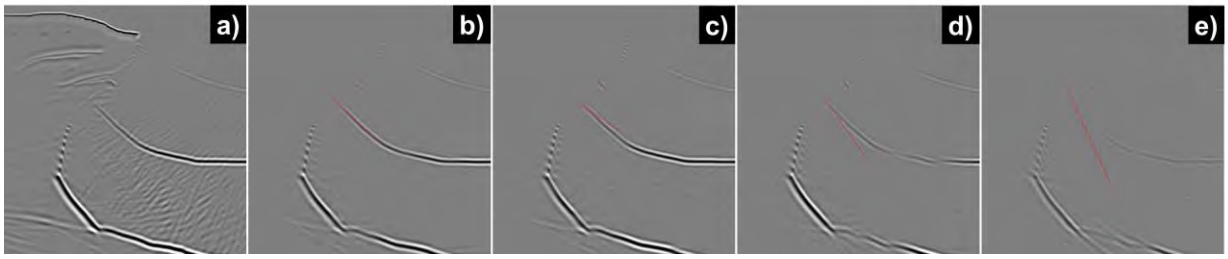

Figure 4 *RTM stack image. (a) Full input. (b) Selective input on horizon with correct dip. (c) Selective input on horizon with wrong dip, 10º flatter than true dip. (d) Selective input on horizon with wrong dip, 10º steeper than true dip. (e) Selective input on horizon with wrong dip, 20º steeper than true dip.*

Acknowledgements

The authors thank CGG for permission to publish this work. We also thank Tony Huang, Nicolas Chazalnoel, and Bin Liu for their thoughtful suggestions and Sophie Feng, Leon Zhu, Jie Chen, and Yuan Yao for working on some of the examples.

References

Chazalnoel, N., Ong, B. and Zhao, W. [2012] Imaging 3-way closures by combining a deconvolution imaging condition with vector offset output RTM. *82nd SEG Annual International Meeting*, Expanded Abstracts, 1-5.

Jin, S. and Xu, S. [2010] Visibility analysis for target-oriented reverse time migration and optimizing acquisition parameters. *The Leading Edge*, **29**, 1372-1377.

Li, Z., Tang, B. and Ji, S. [2012] Subsalt illumination analysis using RTM 3D dip gathers. *82nd SEG Annual International Meeting*, Expanded Abstracts, 1-6.

Mandroux, F., Ong, B., Ting, C., Mothi, S., Huang, T. and Li, Y. [2013] Broadband, long-offset, full azimuth, staggered marine acquisition in the Gulf of Mexico. *First Break*, **31**, 125-132.

Nemeth, T., Wu, C. and Schuster, G. T. [1999] Least-square migration of incomplete reflection data. *Geophysics*, **64**, 208-221.

Shen, H., Mothi, S. and Albertin, U. [2011] Improving subsalt imaging with illumination-based weighting of RTM 3D angle gathers. *81st SEG Annual International Meeting*, Expanded Abstracts, 3206–3211.

Xu, Q., Li, Y., Yu, X. and Huang, Y. [2011] Reverse time migration using vector offset output to improve sub-salt imaging - A case study at the Walker Ridge GOM. *81st SEG Annual International Meeting*, Expanded Abstracts, 3269–3274.